99. Structural Chemistry of Chiral Complexes

NMR and X-Ray Studies on Rh^{I} Compounds of (*S*)-1-[Bis(*p*-methylphenyl)phosphino]-2-[(*p*-methoxybenzyl)amino]-3-methylbutane

by **Heinrich Berger, Reinhard Nesper, Paul S. Pregosin*, Heinz Rüegger,** and **Michael Wörle**

Laboratorium für anorganische Chemie, der Eidgenössischen Technischen Hochschule, ETH-Zentrum, Universitätstrasse 6, CH-8092 Zürich

(12.I.93)

The Rh^{I}(diolefin)complexes [Rh(nbd)(**2**)][PF_6] [Rh(1,5-cod)(**2**)][PF_6], and [Rh((*Z*)-α-acetamidocinnamic acid)(**2**)][PF_6] (**2** = the chiral P,N-ligand (*S*)-1-[bis(*p*-methylphenyl)phospino]-2-[(*p*-methoxybenzyl)amino]-3-methylbutane) have been prepared and characterized. These complexes exist as a mixture of isomers arising from different five-membered-ring conformations and diastereoisomers due to both the prochiral nitrogen and olefin ligands. The three-dimensional solution structures of these complexes have been studied with the specific aim of understanding how the chiral pocket is built. Aspects of the exchange dynamics and their possible relevance to homogeneous hydrogenation are discussed. The solid-state structure for the nbd complex, [Rh(nbd)(**2**)][PF_6], as well as detailed one- and two-dimensional ^{31}P-, ^{13}C-, and ^{1}H-NMR results are presented.

Introduction. – The applications of chiral transition-metal complexes as homogeneous catalysts continue to grow in numbers, and several review articles have appeared [1]. For the metals of the later transition series, the chiral fragment is often a chelating diphosphine, and the resulting complexes have been especially useful in catalytic hydrogenation [2]. Somewhat less studied are complexes containing a chiral mixed coordination sphere, *e.g.* a P,N bidentate ligand, although these are known [3], and, in some cases, quite promising as co-catalysts for specific metal centers. Thus, *Hayashi et al.* [4] have shown that the ligands **1** afford good optical yields in the cross-coupling reactions catalyzed by Pd^{II}. There are additional interesting examples of chiral complexes in catalysis with potentially mixed coordination spheres, although it is not yet completely clear which roles the various ligand atoms play [5] [6].

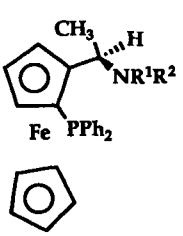

1

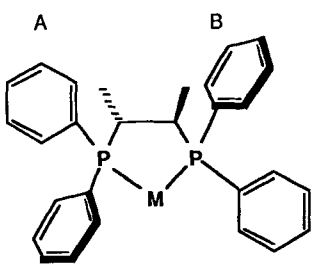

C **D**

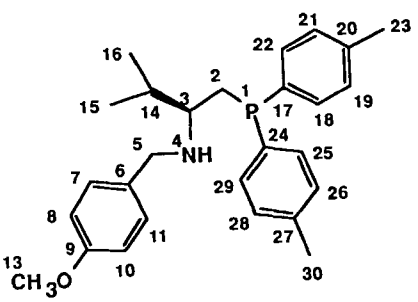

2

The transfer of chirality from the complex to the substrate does not require that the chiral center be close to the metal. It is sufficient that, as a consequence of the chirality, a chiral pocket [7] is formed which then discriminates between the two diastereoisomers. For chiral bidentate phosphines, with Ph end groups, the arrangement of the four aromatic substituents can provide an 'edge-face' array which efficiently transfers the chirality built into the phosphine backbone [8].

It is not immediately clear which of the four Ph groups, A–D, interacts most strongly with incoming and/or coordinated ligands (the Ph groups are usually nonequivalent in a typical complex). With a suitably coordinated organometallic fragment functioning as *reporter* ligand [9], one can use ^{1}H-NOESY methods to define spatial relationships for many parts of the organic shell within the immediate coordination sphere, thereby allowing a rough determination of the solution structure of the complex, in analogy with what has been done for biological substrates [10]. This solution structure in metal complexes represents a 'snapshot' as the various parts of the molecule are not frozen, and segmental rotation plus other movements are, of course, still going on. We have investigated [11] the structures of the two diastereoisomers of the β-pinene-π-allyl binap cationic complex $[Pd(\eta^3\text{-}C_{10}H_{15})((R)\text{- or }(S)\text{-binap})]^+$ and shown that the four distinct Ph groups interact in a very different fashion with the β-pinene-allyl ligand. Within a diastereoisomer, each Ph group is unique, and the two complexes have rather different structures; moreover, the individual differences can be readily demonstrated *via* differences in activation energies for internal motions. Simple calculations have helped to round out our picture of the chiral pockets in these Pd^{II} compounds [11].

In this work, we combine new chemistry and multinuclear NMR spectroscopy in that we report on the coordination and structural chemistry for several Rh^I complexes of our new chiral P,N-ligand, **2**, prepared from (*S*)-valine. Ligand **2** has been deliberately designed so as to allow a ready assignment of the various aromatic protons thereby facilitating their use as NOE probes. This will then permit us to map out the solution structure(s) and chiral pocket(s) associated with its complexes. As we shall show, these measurements demonstrate an unexpected structural flexibility within these Rh^I compounds in terms of intramolecular dynamic processes for complexes of **2** with the result that we can now anticipate the effectiveness of this ligand as co-catalyst in homogeneous hydrogenation.

Results and Discussion. – The Rh^I(diolefin) and Ir^I(1,5-cod) complexes were all prepared, as shown in *Scheme 1* from the corresponding Cl-bridged dimeric complexes.

Scheme 1

$$[M_2Cl_2(\text{diolefin})_2] + 2\,(\mathbf{2}) \xrightarrow[CH_2Cl_2]{2\,K[PF_6]\text{ in acetone/}H_2O} 2\,[M(\text{diolefin})(\mathbf{2})][PF_6] + 2\,KCl$$

M = Rh, diolefin = nbd (**3**)
M = Rh, diolefin = 1,5-cod (**4**)
M = Ir, diolefin = 1,5-cod (**5**)

The formulation of these complexes is supported by elemental analysis and FAB-MS combined with ^{1}H-, ^{13}C-, and ^{31}P-NMR spectroscopy. The solid-state structure of complex **3** has been determined by X-ray diffraction.

1. *X-Ray Structure of [Rh(nbd)(2)][PF$_6$]* (**3**). One aim of the crystal-structure analysis for this complex was to assess how ligand **2** coordinates and specifically, which of the possible five-membered ring conformations and/or diastereoisomers (with respect to the N-coordination) is favored. The five-membered ring-conformation in [PdCl$_2$(**2**)] has been previously shown by us [12] to contain a pseudo-axial i-Pr group in solution, but a pseudo-equatorial i-Pr group in the solid-state. Our calculations [12] on these Pd complexes show only small differences in energy between some of the possible conformers and diastereoisomers; nevertheless, experimentally, we find only one isomer in solution [12].

A selection of interatomic distances and angles for [Rh(nbd)(**2**)][PF$_6$] (**3**) is given in *Table 1*. As shown by the ORTEP plot in *Fig. 1* for complex **3**, the chelate ring adopts a

Table 1. *Selected Bond Lengths* [pm] *and Bond Angles* [°] *for* **3**

Bond lengths [ppm]				Bond angles [°]			
Rh–C(35)	210(1)	P(1)–C(24)	180(1)	C(35)–Rh–N	168.3(4)	C(17)–P(1)–C(24)	105.1(5)
Rh–C(34)	214(1)	P(1)–C(17)	183(1)	C(35)–Rh–P(1)	103.2(3)	C(24)–P(1)–C(2)	108.2(6)
Rh–N	218(1)	P(1)–C(2)	185(1)	C(34)–Rh–N	151.0(4)	C(17)–P(1)–C(2)	105.3(5)
Rh–C(32)	224(1)			C(34)–Rh–P(1)	101.2(3)		
Rh–C(31)	224(1)	N–C(3)	150(1)	N–Rh–C(32)	99.7(5)	C(3)–N–C(5)	112.9(9)
Rh–P(1)	226.7(3)	N–C(5)	150(1)	N–Rh–C(31)	106.3(5)		
Rh–C(33)	279(1)			N–Rh–P(1)	83.1(3)		
Rh–C(36)	282(1)	C(31)–C(32)	136(2)	C(32)–Rh–P(1)	157.7(4)		
		C(34)–C(35)	139(2)	C(31)–Rh–P(1)	163.8(4)		

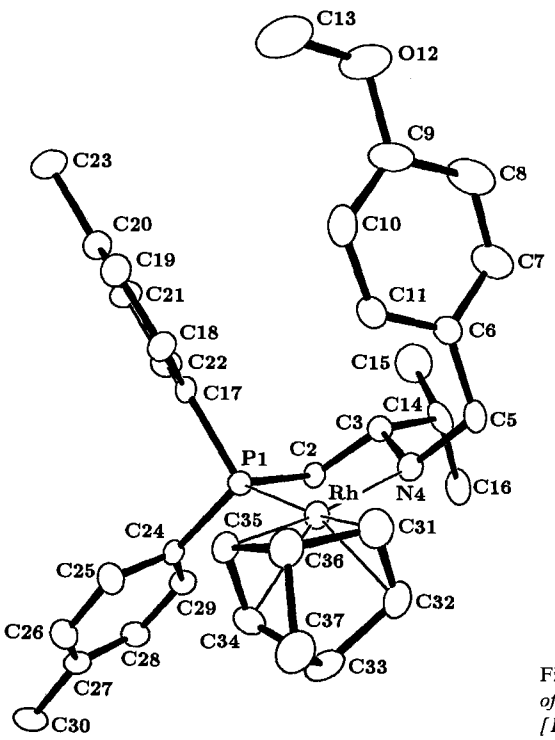

Fig. 1. *ORTEP Plot* [44] *of the cation of [Rh(nbd)(2)][PF$_6$]* (**3**)

conformation in which the i-Pr group is pseudo-equatorial. The *N*-benzyl C-atom is also pseudo-equatorial, with the benzyl aromatic moiety and the axial Ph group of the P(*p*-Tol)$_2$ fragment on the same side of the molecule. Both of these features were also found in the solid-state structure of [$PdCl_2$(**2**)]. If one defines a plane containing the Rh-, N-, and P-atoms, or a mean plane for the Rh-, P-, N-, C(2)-, and C(3)-atoms (values for the latter plane in brackets), then the methine i-Pr C-atom, C(14), is *ca.* 13 (6) pm below and the *N*-benzyl C-atom C(5) *ca.* 38 (65) pm above these respective planes. These values are consistent with the assignment of pseudo-equatorial positions to these substituents. The *ipso*-tolyl C-atoms C(17) and C(24) are *ca.* 160 (190) and 113 (179) pm, above and below the plane, respectively, and are assigned as pseudo-axial and equatorial, respectively. The norbornadiene, nbd, is asymmetrically bound to the Rh-atom, as expected for a diolefin coordinated opposite to a bidentate ligand with two donors of differing *trans*-influence. However, the nbd asymmetry, with respect to the metal, is somewhat more pronounced than that expected for electronic effects alone, as shown in *Scheme 2*. If

Scheme 2[a])

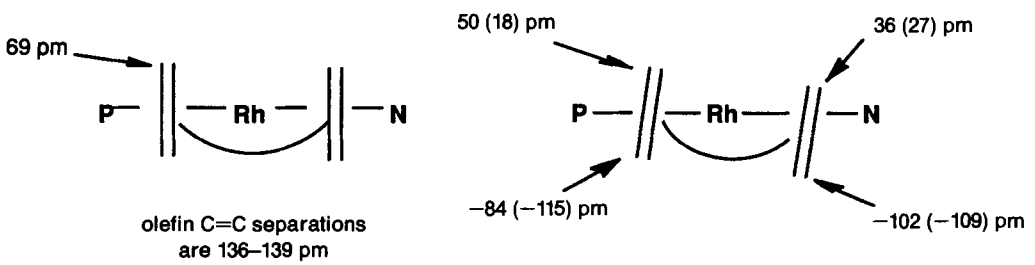

[a]) Values are relative to either P–Rh–N plane or, in parentheses, a mean plane derived using Rh, P, N, C(2), and C(3).

the P–Rh–N plane were to bisect the diolefin, one would expect the four C-atoms to be *ca.* 69 pm from this plane, based on the observed C–C distances of *ca.* 136–139 pm. These separations of the olefinic C-atoms are consistent with somewhat elongated double bonds. In fact, the positions of these four C-atoms suggest that the diolefin has undergone a slight clockwise rotation, combined with a 'slip' which drops the diene down and away from the equatorial *p*-tolyl group. It is likely that this latter distortion arises from the various steric effects associated with the relatively large substituents on both P- and N-atoms.

Although the Rh–C(olefin) distances are not significantly different, the observed separations are consistent with what one has come to expect [13–15] from the differences in *trans*-influence between P and N-donors, with the former being relatively large. Our values for Rh–C(*trans* to P) of *ca.* 224 pm are in good agreement with the values of 217–224 pm found [16] in a series of [Rh(nbd)(P^P)](ClO_4) complexes, where P^P denotes different ferrocene phosphine chelate ligands.

Interestingly, the Rh–P separation, 226.7(3) pm, is on the short side, and in *Table 2*, we show this bond length together with some reference data [16–22]. The Rh–N bond distance, 218(1) pm, is somewhat long when compared with the value of *ca.* 212 pm

Table 2. *Selected X-Ray Literature Data for [Rh(Olefin)(chelate phosphine)]*

Complex	Rh–P Bond length [pm]	Chelate angle P–Rh–P	Literature
[Rh(nbd)(**2**)][PF_6]	227(1)	83.1(3)°	This work
[Rh(cod)(chiraphos)][ClO_4]	228(1)	83.82(6)°	[20]
	227(1)		
[Rh(nbd)(cycphos)][ClO_4]	229(2)	84.1(6)	[8c]
[Rh(mac)(chiraphos)][a])	229(1)	83.1	[21]
ClO_4	223(1)		
[Rh(mpaa)(dipamp)][BF_4][a])	227(1)	83.1	[22]
	224(1)		

[a]) mac and mpaa are bidentate olefin-carbonyl ligands.

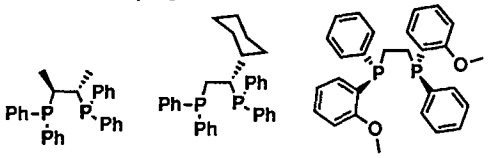

chiraphos cycphos dipamp

found [23] in [Rh(nbd)$(NH_3)_2$]$^+$, and even longer than that observed [24] for the secondary amine Rh–N distance, 209.8(3) pm, in *trans*-[RhCl$(C_2H_4)(C_5H_{10}NH_2)_2$]. The chelate bite-angle of *ca.* 83° is normal for a five-membered ring.

Given the above observations with respect to the diene bonding, it was interesting to ask where the P,N-chelate intrudes into the diene coordination sphere, or put differently, where one finds short interligand contacts. To this end, we have placed the protons in their expected positions at 108 pm from the C-atoms and estimated the corresponding proton-proton separations. These results show that an *ortho*-proton of the equatorial P–(*p*-tolyl) moiety can come within *ca.* 250–260 pm of both olefin protons *cis* to the P-atom, whereas a corresponding *ortho*-proton of the axial P–(*p*-tolyl) group comes to within *ca.* 280 pm of just one of these two olefinic protons. Similarly, the *ortho*-proton adjacent to the N-benzyl C-atom comes within *ca.* 290 pm of an olefinic proton *cis* to the N-ligand. Consequently, although the diolefin has twisted and slipped, the olefinic protons are still relatively close to the equatorial P–(*p*-tolyl) moiety. There are also some relatively close intraligand contacts between the aromatic benzyl protons and the aromatic axial P–(*p*-tolyl) protons. Interestingly, the shortest H,H distances (220 and 224 pm) are *intermolecular* and arise due to contacts between the protons of the MeO C-atom C(13) and C(35) with those of the protons on the Me group C(30) and C(33), respectively. Although all of these H,H contacts are clearly only estimations, they are useful in helping us to understand the multitude of cross-relaxation processes observed in solution *via* NMR spectroscopy.

2. *Solution Structures and NMR Spectroscopy for the Diene Complexes.* The ^{31}P-NMR spectrum for **3**, reveals the presence of two complexes in solution, in the ratio 9.4:1, both of which have $^1J(^{103}Rh,^{31}P)$ values of *ca.* 173 Hz (and consequently have the metal in the +1 oxidation state [25]) but rather different chemical shifts, 35.3 and 28.0 ppm, respectively. As we were aware of the possibility of diastereoisomers (the N-atom is a stereogenic center) and/or conformational isomers (as mentioned above), we

Table 3. *^{1}H-NMR Data for* **3**

Proton	Major isomer in [Rh(nbd)(**2**)][PF_6] (CD_2Cl_2, 500.13 MHz)	Minor isomer in [Rh(nbd)(**2**)][PF_6] (CD_2Cl_2, 500.13 MHz)
H–C(2)	*ca.* 2.25[a]) (*m*, 2 H)	*ca.* 2.38[a]); 2.70
H–C(3)	*ca.* 2.15[a]) (*m*, 1 H)	3.05
NH, H–C(5)	3.80 (*d*, 1 H); 3.66 (*m*, 1 H); 3.92 (*m*, 1 H)	*ca.* 3.80[a])[b]); 3.25[b]); *ca.* 3.90[a])[b])
H–C(7,11)	7.74 (*m*)	7.63
H–C(8,10)	6.90 (*m*)	7.08
CH_3O	3.81 (*s*)	3.88
H–C(14)	2.14 (*m*)	2.05
CH_3	0.77 (*d*); 0.95 (*d*)	1.07; 1.18
H–C(18,22)	7.49 (*m*, *ortho*, axial)	–
H–C(25,29)	7.18 (*m*, *ortho*, equat.)	–
H–C(19,21)	7.33 (*m*)	–
H–C(26,28)	7.26 (*m*)	–
CH_3(*p*-tolyl)	2.36 (*s*); 2.41 (*s*)	2.38; 2.47
H(olefin)	3.90[c]) (*s*, 1 H)	3.33
H(olefin)	4.16[c])[d]) (*d*, 1 H)	3.50
H(olefin)	4.90[e]) (*d*, 1 H)	*ca.* 3.93[a])
H(olefin)	5.66[e])[f]) (*s*, 1 H)	5.43
H–C(nbd)	4.02, 4.04 (*d*, 2 H)	3.5, 3.81
CH_2(nbd)	1.53, 1.59 (*q*, 2 H)	1.2, 1.4

[a]) Overlapping signals. [b]) Assignment suggested by COSY, but not certain. [c]) *trans* to NH. [d]) Close to axial *p*-tolyl. [e]) *trans* to P. [f]) Close to NH.

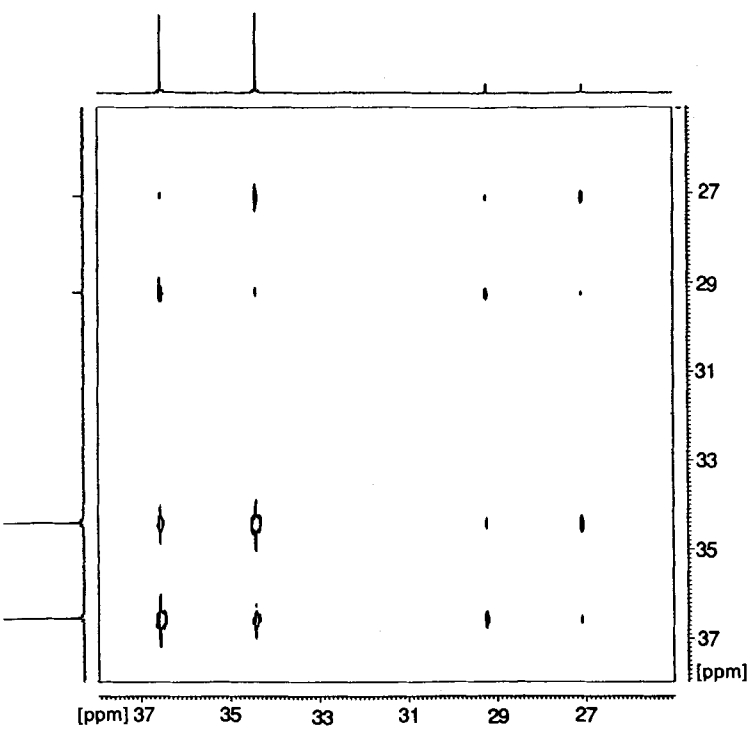

Fig. 2. *2D-^{31}P-Exchange NMR spectrum* (101.25 MHz) *for [Rh(nbd)(**2**)][PF_6]* (**3**)

have measured the 2-D ^{31}P-exchange spectrum [26–28], and this is shown in *Fig. 2*. The pronounced cross-peaks indicate that these two complexes are indeed in equilibrium.

Further details of the dynamics arise from a phase-sensitive 2-D ^{1}H-NOESY measurement [29–33]. In this methodology, cross-peaks with the same sign as the diagonal are due to exchange, whereas cross-peaks with the opposite sign arise from NOE (assuming that the extreme narrowing condition is still valid [34]). Although the ^{1}H-NMR spectrum of the mixture is not trivial, even at 500 MHz, many of the signals are assignable (see *Table 3*). Consequently, the *exchange* peaks, indicated in *Fig. 3*, reveal *two* processes: exchange between the two complexes, as found in the ^{31}P experiment, and a selective intramolecular exchange between pairs of the four olefinic protons of the nbd within a complex. Specifically, each of the olefinic protons *trans* to the N-atom exchanges with just one of the olefinic protons *trans* to the P-atom. To appreciate these dynamics, we must now turn to the structures of these complexes.

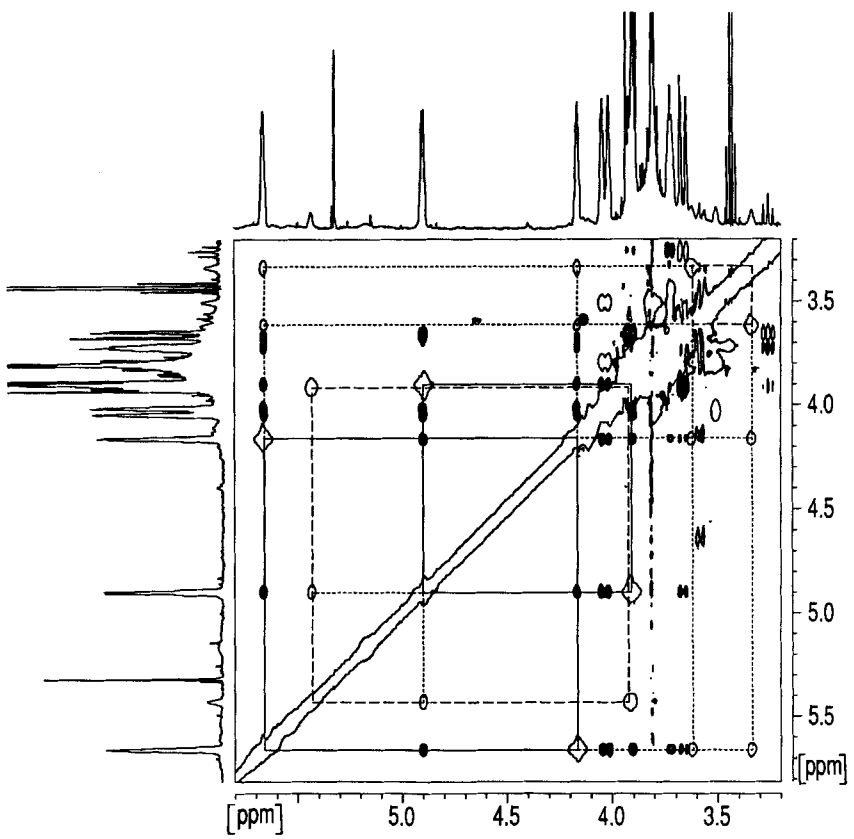

Fig. 3. *Section of the 2D ^{1}H-NOESY spectrum for [Rh(nbd)(2)][PF$_6$] recorded in CDCl$_3$ at 500.13 MHz.* The diagonal and the cross-peaks due to chemical exchange are distinguished from the NOE peaks by drawing only a single contour line. The intramolecular exchange of the olefinic protons is indicated by squares drawn in full for the major isomer and dashed lines for the minor isomer. Intermolecular exchange between the two isomers is shown *via* the dotted lines.

In deciding whether the complexes were conformational or diastereoisomeric isomers, we have considered aspects of their ^1H and ^{13}C characteristics. We were especially interested in the values $^3J(^{31}P,^1H)$ and $^3J(^{31}P,^{13}C)$ due to the known dependence [35–37] of these spin-spin couplings on dihedral angle. In our previous study [12], we showed that an axial i-Pr group (and consequently equatorial H–C(3)) gave $^3J(^{31}P,^1H)$ values > 30 Hz. This corresponds to the relatively large dihedral angle shown in **6**.

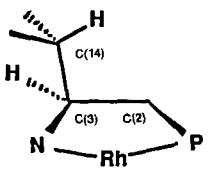

6

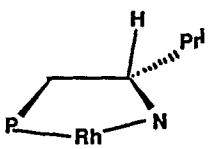

7

Fortunately, we have been able to estimate the $^3J(^{31}P,^1H–C(3))$ value in both isomers: in the major isomer *via* analysis [38] of a CH cross-peak (from the corresponding correlation) and in the minor isomer *via* the analysis of the corresponding COSY cross-peak (*Fig. 4*). In essence, we are using the second dimension to resolve signals not readily

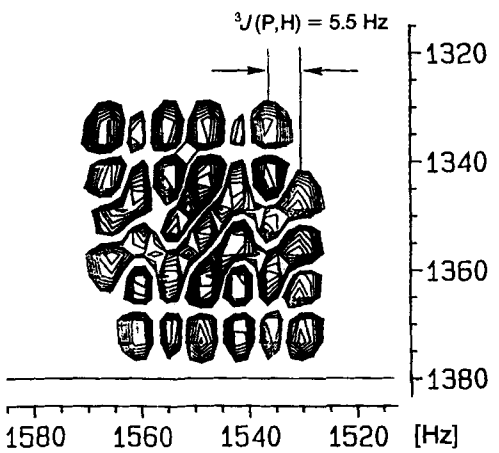

Fig. 4. *^1H-COSY Cross-peak for the proton H–C(3) showing high-resolution features which allow the determination of $^3J(P,H)$ in [Rh(nbd)(2)][PF_6]* (3)

interpretable in the conventional 1-D mode. In the major isomer, this value is not directly measurable, but certainly < 10 Hz, whereas in the minor complex the value is *ca.* 5.5 Hz, so that in both of these compounds we are dealing with a pseudo-equatorial i-Pr group, *i.e.* **7**. Therefore, the two complexes form as a consequence of the N-coordination, and we are dealing with diastereoisomers with structural fragments related to **8** and **9**.

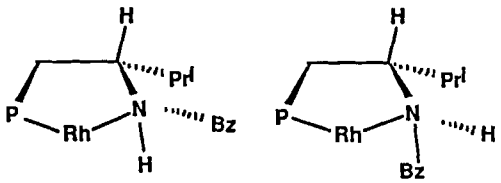

8 **9**

The choice between **8** and **9** can be made using NOE's: in the *minor* isomer our observed ^3J(NH,H–C(3)) value of *ca.* 3 Hz, indicates [39] that this isomer has structure **9**, and, therefore, the major isomer, structure **8**.

The solution structure and shape of the chiral pocket for the major isomer can now be readily deduced using the NOESY results. The axial NH of the major isomer shows a moderate NOE to an nbd olefin proton *trans* to the P-atom. The *N*–Bz (Bz = *p*-methoxybenzyl) *ortho*-protons interact strongly with the *other* olefinic proton *trans* to the P-atom so the Bz group is on the other side of the molecule relative to the NH. The two types of P–(*p*-Tol)$_2$ *ortho*-proton are well resolved, and one of these interacts with the *ortho*-protons of the N–Bz. Together, these data allow us to assign the pseudo-axial and pseudo-equatorial *ortho*-P–(*p*-tolyl) resonances and place these in space as shown in **10**.

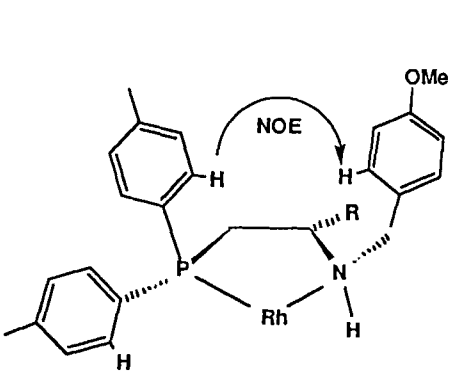

10 R = i-Pr

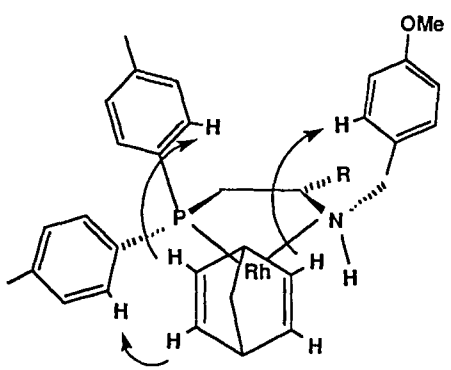

11 R = i-Pr

Finally, we can use our knowledge of the positions of these *ortho*-protons to assign the four individual olefinic protons of the nbd, as shown in **11** (for clarity only three contacts are shown). The final picture, in this case, is essentially that found in the solid-state *via* X-ray diffraction.

The ^{13}C-NMR characteristics for **3** are very useful; however, we emphasize the ^{31}P coupling to the i-Pr methine, $^3J(^{31}P,^{13}C(14))$, which, at 13 Hz, is relatively large and a valuable probe for the ring conformation. This empiricism is based on literature [35–37] for four-coordinate P compounds as well as on observations made by one of us [40] for PCy_3 complexes in which the ^{31}P is in an equatorial position.

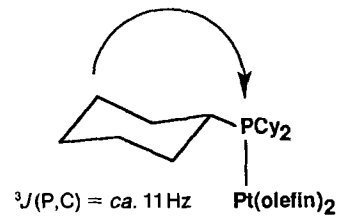

Consequently, 13 Hz suggests an equatorial i-Pr group, in keeping with our proton results. This empirical tool will be used below, where key protons are not readily assigned. The most important ^{13}C signals, including the four different olefin C-atoms of the nbd, can be readily assigned *via* a $^{13}C,^{1}H$ correlation. Before returning to the dynamics, we note that the chiral pocket, both in the solid and in the solution, is rather open in the area around the N-atom.

Now that we know the position of each important proton, we can reconsider our observed intramolecular dynamics and postulate nbd rotation as a source of the second process. The proton-exchange spectroscopy clearly shows that (referring to **11**) the 'upper-left' and 'lower-right' (and of course the 'upper-right' and 'lower-left') olefinic protons are involved in the specific exchange process. This is easily understood, if the olefin is allowed to rotate, and we can now rationalize both the inter- and intramolecular dynamics assuming that *a*) the N-ligand dissociates to afford a three coordinate (or solvent-stabilized four-coordinate) complex; *b*) subsequent inversion at the N-atom occurs; *c*) the N-atom coordinates again (*Scheme 3*).

Scheme 3

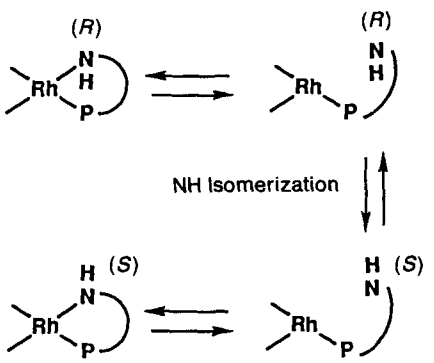

If, during the lifetime of the three-coordinate species, the olefin is allowed to rotate, recombination before inversion can account for the intramolecular process. Olefin rotation might occur in a five-coordinate complex; however, such a five-coordinate species (formed by addition of solvent or adventitious H_2O) would not account for the exchange between diastereoisomers. We note here that diolefin rotation has been observed previously in Rh^{I}- and Ir^{I}(cyclooctadiene) complexes [40b] [41].

There are, of course, other possibilities. After nitrogen dissociation, the initial three-coordinate T-shaped species could rearrange to a new T-shaped complex (with P now

trans to the other C=C bond). Rotation around the Rh–P bond, followed by N recoordination would also be consistent with our results. This mechanism avoids cleavage of two Rh–olefin bonds, but still requires initial Rh–N bond breaking. At present, we are unable to distinguish between these possibilities.

We have made similar NMR studies on the complex [Rh(1,5-cod)(**2**)][PF_6] (**4**), and we find two isomers in solution in the ratio 10:1 with $^1J(^{103}Rh,^{31}P)$ values of 156 and 158 Hz, and δ values of 37.3 and 28.0, respectively. Moreover, based on ^{1}H-NOESY studies, we find essentially the same behavior in terms of the dynamics. Although the four CH_2 groups of the cod make the ^{1}H spectrum somewhat less accessible for our methods, based on a detailed analysis of the ^{1}H-NOESY cross-peaks, we believe that the structures of the two isomers observed for **4** correspond to those for **3**. Moreover, $^3J(^{31}P,^{13}C(14)) = 11$ Hz, in the major isomer, suggesting a pseudo-equatorial i-Pr group.

Table 4. *^{1}H-NMR Data for* **4**

Proton	δ[a])	Proton	δ[a])
H–C(2)	2.30, 2.45[b]) (*m*)	CH_3(*p*-tolyl)	2.36, 2.45 (*s*)
H–C(3)	2.3–2.4[b]) (*m*)	–	–
NH	4.12 (*s*)	H(olefin)	3.34[c])
H–C(5)	3.75, 4.01 (*m*)	H(olefin)	3.98[c])
H–C(7,11)	7.66 (*m*)	H(olefin)	4.77[d])
H–C(8,10)	6.87 (*m*)	H(olefin)	5.62[d])
CH_3O	3.82 (*s*)	CH_2(cod)[b])	1.82, 2.25 (*m*)
H–C(14)	2.14 (*m*)	CH_2(cod)[b])	2.1, 2.25 (*m*)
CH_3	0.75, 1.00 (*m*)	CH_2(cod)[b])	2.68, 2.37 (*m*)
		CH_2(cod)[b])	2.25, 2.81 (*m*)

[a]) $CDCl_3$, major isomer, 7.63, *ortho*-protons (axial *p*-tolyl); 7.34, *meta*-protons (axial *p*-tolyl); 7.24–7.27, arom. H of equatorial *p*-tolyl.

[b]) Considerable overlap makes assignment tentative.

[c]) *trans* to N, 3.34 proton in contact with pseudo-equatorial *p*-tolyl.

[d]) *trans* to P, 5.62 proton close to NH, 4.77 close to benzyl.

As planned, we have a picture of the chiral pocket, when **2** coordinates to Rh^I, and this reveals crowding in the region of the equatorial P–(*p*-tolyl) group; however, the dynamics have provided us with a clue as to an unexpected, indeed undesirable, lability associated with these materials, since the chiral pocket is readily lost when the nitrogen dissociates.

We have also prepared the complex [Ir(1,5-cod)(**2**)][PF_6]. This compound shows *four* complexes in solution, and we give the appropriate ^{31}P-NMR data in the *Exper. Part.* Although we have not attempted to characterize these isomers further, the presence of four complexes is potentially interesting, and we shall return to this point in the next section.

3. *Solution Structures and NMR Spectroscopy for the Rh^I Complex with Cinnamic Acid.* Given the interest in catalytic hydrogenation, we have considered the reaction of **3** with 1-atm H_2 in the presence of 1 equiv. of the cinnamic-acid derivative, AC (*Scheme 4*).

Scheme 4

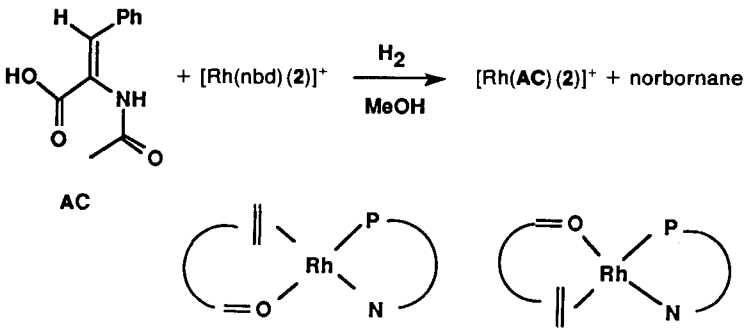

Possible geometric isomers

Apart from the presence of norbornane (and some norbornene), confirmed *in situ via* ^{13}C-NMR, the ^{31}P-NMR spectra of the reaction mixture, **12**, showed the presence of five components, several of which slowly disappeared over a period of several hours. *Table 5* shows the various amounts of the three main materials as a function of time. Given the slow changes observed, it is not surprising that a ^{31}P 2-D-exchange spectrum of the end products, showed *no* cross-peaks so that these materials are presumably exchanging very slowy or not at all on the NMR time scale. Given the similarity of the ^{31}P-NMR data for the two remaining complexes after several days ($\delta = 55.5$, $^1J(^{103}\text{Rh},^{31}\text{P}) = 174$ Hz; $\delta = 57.6$, $^1J(^{103}\text{Rh},^{31}\text{P}) = 174$ Hz), it was likely that we were, again, concerned with isomers.

Table 5. *^{31}P-NMR Data for* **12** *as a Function of Time*

Time	^{31}P-NMR		J(Rh,P) [Hz]	Rel. abundance [%] (*via* ^{31}P-NMR)
10 min	**A**	55.5	174	30
	B	57.6	174	63
	C	49.0	174	7
30 min	**A**	55.5	174	40
	B	57.6	174	54
	C	49.0	174	6
3 d	**A**	55.5	174	86
	B	57.6	174	14
5 d and 7 d	**A**	55.5	174	90
	B	57.6	174	10

The ene-amide ligand is recognized [21] [22] to function as an oxygen-olefin chelate so that initially we considered the possibility of geometric isomers, as suggested by the structures sketched in *Scheme 4*. This could be disproven *via* an analysis of the various ^{31}P- and ^{13}C-NMR characteristics. Specifically, the four ^{13}C olefinic signals, detected at a time when both isomers are relatively abundant, are observed at $\delta = 70.7$ and 75.8 for one isomer, and $\delta = 71.5$ and 75.0 for the second, with the latter two absorptions diminishing as a function of time. Since ^{13}C signals for Rh-coordinated olefins *trans* to a tertiary

phosphine are found at much lower field, as shown by the model complexes **3** and **4** and the literature [42], we are dealing with isomers having the coordinated olefins *cis* to the P-donor. The lower-field resonances are quaternary, and the higher field signals of =CH type C-atoms as shown by DEPT methods. One would have made the same C assignments using the $^2J(^{31}P,^{13}C(olefin))$ and $^1J(^{103}Rh,^{13}C)$values.

Of the selected ^{13}C-NMR data shown in the *Exper. Part*, we note that those for the i-Pr methine C-atom C(14), $\delta = 26.4$, $^3J(^{31}P,^{13}C) = 14$ Hz (major) and $\delta = 30.4$, $^3J(^{31}P,^{13}C) = 4.7$ Hz (minor), are immediately informative and suggest that, in contrast to the situation for **3** and **4**, we have different ring conformations in **12**. In this case, the major isomer has the i-Pr group pseudo-equatorial. Support for very different i-Pr groups is especially evident from the ^1H-NMR data (*Table 6*) in that the Me signals appear at $\delta = 0.73$ and 0.88 in the major, and $\delta = 0.26$ and 0.57 in the minor isomer.

Table 6. *^1H-NMR Data[a]) for the Isomers* **A** *and* **B** *of* **12**

	Isomer **A**	Isomer **B**
H–C(2)	2.28[b]) (*m*)	2.75 (*m*)
	2.53[b]) (*m*)	2.45 (*m*)
H–C(3)	*ca.* 2.47[b]) (*m*)	2.67 (*m*)
H–C(5)	3.73 (*d*); 4.25 (*d*)	4.03 (*d*); 4.15 (*d*)
H–C(8,10)	6.93 (*m*)	6.71 (*m*)
H–C(7,11)	7.56[b]) (*m*)	7.30[b]) (*m*)
H–C(14)	*ca.* 2.46 (*m*)	1.50 (*m*)
CH_3	0.73 (*d*); 1.02 (*d*)	0.26 (*d*); 0.58 (*d*)
CH_3(*p*-tolyl)	2.34 (*s*)	2.40, 2.41 (*s*)
H–C(2')(olefin)	4.23 (*m*)	4.41 (*m*)
Acyl group	2.06 (*s*)	2.23 (*s*)
CH_3O	3.88 (*s*)	3.76 (*s*)
H–C(19,21)	7.06 (*m*, *meta*, axial)	
H–C(26,28)	7.21 (*m*, *meta*, equat.)	

[a]) CD_3OD, 500.13 MHz, NH proton not observed. [b]) Overlapping signals.

There are also large differences in the chemical shifts for the i-Pr methine protons. Presumably, these differences in chemical shift are anisotropic in origin and reflect the differing proximities to the various aromatic moieties, especially when the i-Pr is pseudo-axial. Further, $^3J(^{31}P,^1H\text{-}3)$ in the minor isomer is *ca.* 30 Hz, thus pointing to an '*anti*'-orientation of these spins as in **6**. Consequently, we assign the major isomer a conformation as in **7** and the minor a conformation as in **6**. Our calculations [12] for Pd complexes of **2** have shown only small energy differences between the conformers having $(i\text{-}Pr)_{eq}$ $(N\text{–}Bz)_{eq}$ *vs.* $(i\text{-}Pr)_{ax}$ $(N\text{–}Bz)_{ax}$ so that our observations in **12** need not be surprising.

For both isomers, the assignment of the N configuration and the decision as to the coordinated olefin-face follow from detailed considerations of the ^1H-NOESY data (see *Scheme 5*). The most important interactions are summarized below.

Major Isomer. 1) Both CH's (H–C(3) and Me_2CH) show strong NOE's to the *ortho*-protons of the N–Bz, suggesting an equatorial N–Bz moiety which spends most of its time 'above' the i-Pr group ('above' and 'below' refer to the P–Rh–N plane, viewed from behind the coordinated olefin ligand). *2*) The MeO group, which seems remote, has a strong contact to one of the *meta*-protons of the *p*-tolyl groups, an indication that this

Scheme 5

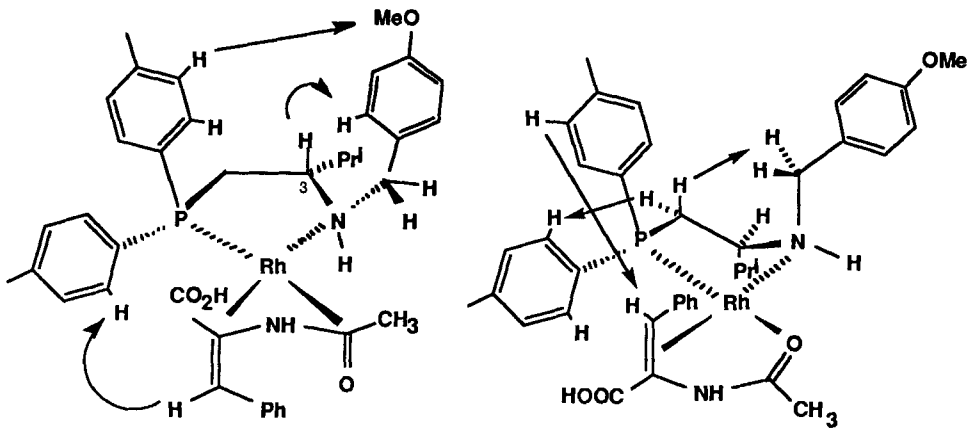

latter is 'above' as shown in *Scheme 5*. *3*) No NOE from any of the N–Bz protons to the PCH_2, again suggesting the N–Bz is equatorial. *4*) The *meta*-protons of the second *p*-tolyl show another strong NOE to the olefin CH=C, thereby placing this proton 'down' and thus defining the coordinated olefin face. A section of the ^{1}H-NOESY for **12** is given in *Fig. 5*. It is interesting to note that the structure has been 'solved' without using the *ortho*-protons of the group P–(*p*-tolyl) protons as we usually do.

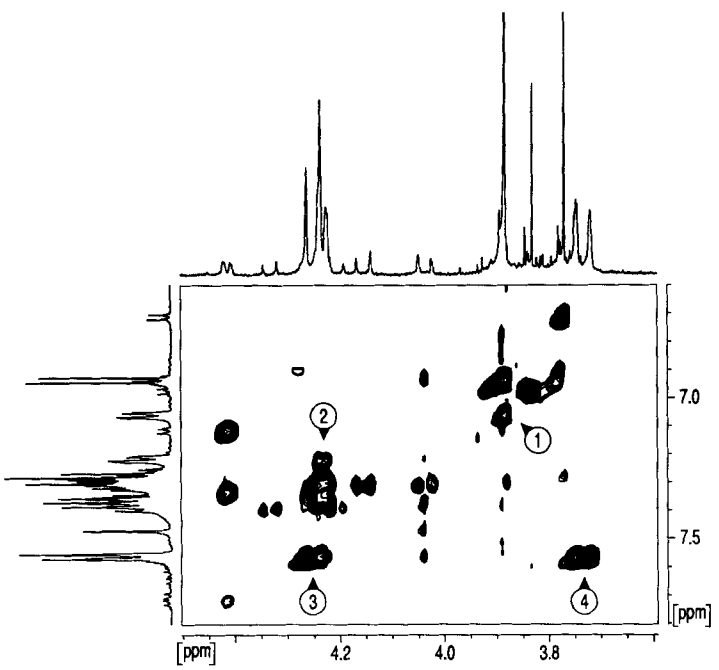

Fig. 5. *Section of the 2D ^{1}H-NOESY spectrum for [Rh(AC)(2)][PF$_6$] showing selected NOE's arising from the aromatic region of the spectrum* (500.13 MHz). Cross-peaks noted arise from: ① MeO to *meta*-H of the *p*-tolyl ring; ② AC olefin H to *meta*-H of the second *p*-tolyl ring; ③ and ④ benzyl CH_2's to *ortho*-H's of N–Bz ring.

Minor Isomer. 1) A strong NOE from the axial Me_2CH methine proton to the *ortho*-protons of a *p*-tolyl group defines this tolyl as lying 'below'. *2*) This same *ortho*-proton of the tolyl group shows a strong interaction to one of the P–CH_2 protons. *3*) The other P–CH_2 proton interacts strongly with the N–CH_2 protons. This is strong support for an axial N–Bz group, since an equatorial N–Bz would have the N–CH_2 protons remote from the P–CH_2 (points *2* and *3* help to define 'above and below', since we know the i-Pr group is axial). *4*) The *meta*-protons from the remaining *p*-tolyl group show a relatively strong NOE to the olefin CH=C, thereby revealing that the other olefin face is coordinated in the minor isomer.

4. *Further Comments.* It is interesting that the structures we find with **12** do not involve N diastereoisomers. Either one epimer is formed preferentially or the two are in fast equilibrium as a consequence of nitogen dissociation followed by inversion and recombination as mentioned in connection with **3**. The subject remains open[1]). It is of note that **12** does not react further with H_2 under these relatively mild conditions. The cod complex **4** also reacts with H_2 in the presence of our cinnamic acid derivative, as described for **3**, to again give **12**, suggesting some inherent additional stability for **12** or a higher activation energy barrier for the reduction of the coordinated ene-amide.

Given all of the unexpected lability mentioned above, interconversion of isomers, lack of conversion of **12**, *etc.*, we were not surprised to find that **3**–**5** were of limited utility with respect to the hydrogenation of our chosen cinnamic acid substrate. Details on these studies are given in *Table 7* and the *Exper. Part.* There is some hydrogenation under

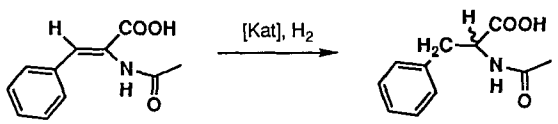

Table 7. *Hydrogenation Results*

Catalyst mol-% Complex	Solvent	H_2 pressure	Temp., time	Product yield[a]) [%]
[Rh(nbd)(**2**)][PF_6] 5%	MeOH/H_2O 10:1	1 bar	r.t., 8 h	0
[Rh(nbd)(**2**)][PF_6] 5%	MeOH/H_2O 10:1	1 bar	60°, 3 h	37
[Rh(cod)(**2**)][PF_6] 5%	MeOH/H_2O 10:1	1 bar	60°, 3 h	45
[Ir(cod)(**2**)][PF_6] 5%	MeOH/H_2O 10:1	1 bar	60°, 3 h	38
[Rh(cod)(**2**)][PF_6] 5%	MeOH/H_2O 10:1	20 bar	r.t., 4 h	45

[a]) Followed *via* ^{1}H-NMR in CD_3OD, < 5% ee in all cases (*via* GC).

relatively mild conditions; however, the reaction was slow and we observed finite quantities of a black solid (metallic rhodium?) which makes it impossible to be certain that the reaction is, indeed, homogeneous; consequently, further discussion on this topic seems presumptuous.

Conclusion. – It is clear that our approach allows us to determine the 'solution structures' of our chiral Rh^I(olefin) complexes. Within this phrase, we understand not

[1]) We do note that there was a complex 'C' which disappeared slowly, suggesting relatively slow kinetics for the interconversion (if, indeed, C is an epimer). Moreover, for the Ir^I complex **5** we find a number of NMR signals which might arise due to diastereoisomers. If the Rh kinetics with **12** are relatively slow, perhaps the Ir kinetics are even slower with the result that we observe these compounds in solution.

only the relative geometries of the donor atoms but *a*) the conformation of the five-membered ring *b*) the configuration at the N-center, and *c*) the stereochemistry associated with olefin coordination, *i.e. re* or *si* face complexation. It seems obvious that these methods are not intended to replace diffraction studies, but rather supplement them. The solution measurements have the advantage that we can obtain detailed structural information on pairs of isomers, despite significant population differences. An additional bonus stems from the capability of 2-D NOESY methods to simultaneously obtain distance and exchange information. When taken together, the data allow us to envision the shape of the chiral pocket, and whether it lives long enough to be useful and, therefore, provide hints as to how effective these materials might function as catalysts.

Experimental Part

Crystal Structure. The structure determination was performed on a transparent colorless crystal with well shaped faces. The space group $P2_12_12_1$ is unambiguously determined by the systematic extinctions. The internal consistency of the data ($R_{av.} = 0.028$) is rather good. The structure was solved by direct methods and refined with 426 free parameters and an overdetermination of a factor of five [43]. The H-atom positions were located by geometrical constraints and refined using an overall temperature factor. Crystal data are given in *Table 8*. There

Table 8. *Crystal Data for* **3**

Formula	$C_{34}H_{42}F_6NOP_2Rh$ (759.19)
T[°C]	r.t.
Space group	$P2_12_12_1$-D^4, (Nr. 19)
Lattice constants	$a = 952.6(3)$ pm, $b = 1874.2(4)$ pm, $c = 1940.9(5)$ pm, $V = 3465.07(11)$ Å^3
Z	4
$\rho_{ber.}$ [g cm^{-3}]	1.454
μ [cm^{-1}]	5.67
$\lambda(MoK_\alpha)$	71.069 pm (graphite monochromated)
Tot.	5223
Indep. reflections	2515
$I(hkl) \geq 3\sigma$	2043
R(average)	0.028
R(aniso)	0.052
R_w(aniso)	0.049

was no difficulty in determining the structure of the cation; however, the PF_6^- anion turned out be disordered. This is indicated by the lack of high-order reflections. The F-atoms are distributed over a shell of electron density of a radius $140 \leq r \leq 180$ pm from the center of the P-atom. The P-atom itself shows a rather high isotropic temp. factor, as well, which corresponds to a mean positional variation of *ca.* 30 pm. This allows for all the F-atoms to be at reasonable distances $155 \leq d \leq 165$ pm from the central P-atom. The disordered anion especially influences the neighboring groups of the cation and this is the reason for the relatively large temp. factors of some of the light atoms. Taking into account the fairly high correlations between the F-atom parameters which do not allow for a precise determination of the individual occupancies, they may be interpreted as multiples of 1/5. This gives rise to the assumption that the PF_6^- anion occurs in five different orientations.

NMR Spectroscopy. NMR Spectra were measured on *Bruker AMX-500* and *AC-250* spectrometers. ^{1}H-NOESY Spectra were obtained as described in [9] [11] [29]. C,H Correlations and DQF-COSY spectra were obtained using standard procedures.

Synthesis of [Rh(nbd)(2)][PF$_6$] (**3**). All operations were carried out under Ar. A soln. of KPF_6 (127 mg, 0.7691 mmol) in *ca.* 1 ml of acetone and 2 drops of H_2O, was added to a soln. of di-μ-chlorobis(norbornadiene)rhodium (160 mg, 0.345 mmol) dissolved in *ca.* 5 ml of CH_2Cl_2. Stirring for 5 min was followed by filtration of the KCl and addition of 3 ml of a CH_2Cl_2 soln. of **2** (290 mg, 0.691 mmol). Stirring for an additional 30 min was followed by addition of $MgSO_4$. After removal first of the drying agent and then of the solvent i.v., the crude solid was recrystallized from a minimum of CH_2Cl_2/Et_2O to afford 332 mg (63%) of product. Analysis for $C_{34}H_{42}F_6NOP_2Rh$ (759.18): $[\alpha]_D = 65.5 \pm 1$ ($c = 1.05$, $CHCl_3$). ^{1}H-NMR (500.13 MHz, CD_2Cl_2): *cf. Table 3.* ^{13}C-NMR (major isomer; 62.89 MHz, $CDCl_3$): 14.1 (CH_3); 21.4 (CH_3); 21.5 (C(23, 30)); 26.1 (J(P,C) = 13, C(14)); 28.7 (J(P,C) = 27, C(2)); 51.0 (C(5)); 52.5, 53.4 (C(3′,6′)); 55.3 (C(olefin)); 55.3 (MeO); 61.7 (J(P,C) = 5.7 C(3)); 65.0 (C(olefin)); 66.4 (J(P,C) = 4, C(7′)); 89.7 (C(olefin)); 93.7 (C(olefin)); 114.4 (C(8,10)); 125.5 (C(9)); 129.4 (C(7,10)); 129.9, 130.1 (C(19, 21, 26, 28)); 131.5, 133.6 (C(18, 22, 25, 29)); 141.2 142.5 (C(20, 27)); 159.6 (C(6)). ^{31}P-NMR (101.25 MHz, $CDCl_3$): 35.3 (J(Rh,P) = 173); 28.0 (J(Rh,P) = 174). FAB-MS: 614.1, 570.0, 550.0, 520.0, 499.0, 407.9, 312.9, 223.9, 180.9, 154.0, 121.0, 90.9. Anal. calc. for $C_{34}H_{42}F_6NOP_2Rh$ (759.18): C 53.77, H 5.57, N 1.84; found: C 53.55, H 5.76, N 1.70.

Synthesis of [Rh(1,5-cod)(2)][PF$_6$] (**4**). This complex was prepared as described for **3**, and was recrystallized from a minimum of $CHCl_3/Et_2O$ 1:2: [Rh$_2$(μ-Cl)$_2$(cod)$_2$] (143 mg, 0.290 mmol), ligand **2** (244 mg, 0.580 mmol), KPF_6 (43 mg, 0.580 mmol). Yield: 73%. ^{1}H-NMR: *cf. Table 4.* ^{13}C-NMR (62.89 MHz, $CDCl_3$): 15.3 (CH_3); 20.1 (CH_3); 21.4, 21.6 (C(23, 30)); 27.4 (J(P,C) = 11, C(14)); 30.0, 30.9, 34.1, 34.2 (CH_2 of cod); 29.3 (J(P,C) = 27, C(2)); 52.0 (C(5)); 55.3 (MeO); 63.5 (J(P,C) = 5, C(3)); 72.9 (C(olefin)); 79.3 (C(olefin)); 105.4 (C(olefin)); 108.0 (C)olefin)); 114.3 (C(8, 10)); 125.5 (C(9)); 129.4 (C(7, 11)); 130.1, 130.5 (C(19, 21, 26, 28)); 131.8, 133.7 (C(18, 22, 25, 29)); 141.5, 142.6 (C(20, 27)); 159.6 (C(6)). ^{31}P-NMR (101.25 MHz, $CDCl_3$): 37.3 (J(Rh,P) = 157); 28.0 (J(Rh,P) = 158). FAB: 630.1, 586.0, 550.0, 520.0, 314.9, 223.9, 180.9, 154.0, 121.0, 76.9, 3.43. Anal. calc. for $C_{35}H_{46}F_6NOP_2Rh$ (775.59): C 54.20, H 5.98, N 1.81; found: C 54.32, H 6.07, N 1.62.

Synthesis of [Ir(1,5-cod)(2)][PF$_6$] (**5**). This complex was also prepared as described for **3** and recrystallized from a minimum of CH_2Cl_2/Et_2O: [Ir$_2$(μ-Cl)$_2$(cod)$_2$] (147 mg, 0.218 mmol), ligand **2** (183 mg) (0.437 mmol), KPF_6 (80 mg, 0.437 mmol). Yield: 283 mg (75%). ^{31}P-NMR (101.25 MHz, $CDCl_3$): 37.3 (integral $\approx$ 68%); 17.6 (integral $\approx$ 14%); 13.8 (integral $\approx$ 11%); 13.1 (integral $\approx$ 7%). ^{31}P-Exchange-NMR shows exchange between the main signal at 37.3 and the signal at 17.6 ppm. Anal. calc. for $C_{35}H_{46}F_6NOP_2Ir$ (864.9): C 48.60, H 5.36, N 1.62; found: C 47.83, H 5.39, N 1.50.

In situ *Preparation of* **12**. [Rh(nbd)(**2**)][PF$_6$] (20 mg, 0.014 mmol) and the α-acetamidocinamic acid (2.8 mg, 0.014 mmol) were dissolved in CD_3OD. Stirring for 5 min was followed by bubbling H_2 through the soln. for 10 min. The soln. was transferred to an NMR tube and the reaction monitored *via.* ^{31}P-NMR after 30 min, 3 h, 3 d, and 5 d.

Hydrogenation of the α-Acetamidocinnamic Acid. After flushing the solvent with Ar, the cinnamic acid substrate and catalyst were dissolved and the soln. treated with H_2 for 30 min. Filtration, followed by solvent removal *i.v.*, gave a product mixture which was analyzed *via* ^{1}H-NMR in CD_3OD. In all cases, a black residue was observed. For the 1,5-cod complex, the color change required *ca.* 15 min, whereas with nbd complex the color change was immediate. Selected data are given in *Table 7.*

Reactivity of **3** *with* H_2. This check was made to be certain that the catalyst reacted with H_2. The deuterated solvent shown in *Table 8* was flushed with Ar and then used to dissolve *ca.* 20 mg of **3**. The soln. was then transferred to an NMR tube and the starting material checked *via* ^{31}P-NMR. After transfer to a *Schlenk* tube, the soln. was subjected to 1-atm H_2 for 10 min. The resulting soln. was then studied using ^{31}P-NMR methods. It is worth noting that in all cases the soln. color changed from yellow to red-black on contact with H_2.

Table 9. *^{31}P-NMR-Results from the Reaction of* **3** *with* H_2[a)] [b)]

Solvent	^{31}P-NMR of **3**	^{31}P-NMR of the product
CD_3OD	35.2 (J(Rh,P) = 173, I = 15); 27.7 (J(Rh,P) = 173, I = 1)	49.8 (J(Rh,P) = 123, I = 3); 49.4 (J(Rh,P) = 123, I = 2)
(D_8)THF	35.3 (J(Rh,P) = 175, I = 15); 27.6 (J(Rh,P) = 174, I = 1)	61.8 (J(Rh,P) = 175); 36.8–53.7
$CDCl_3$	35.3 (J(Rh,P) = 173, I = 10); 27.9 (J(Rh,P) = 174, I = 1)	63.6 (J(Rh,P) = 113, I = 1); 60.7 (J(Rh,P) = 116, I = 1)

[a)] Relative intensity, I.

[b)] Obviously, the starting material reacts with H_2 in the absence of substrate.

REFERENCES

[1] R. Noyori, M. Kiramura, in 'Modern Synthetic Methods', Ed. R. Sheffold, Springer Verlag, Berlin, 1989, p. 119; J. M. Brown, *Chem. Brit.* **1989,** 276; W. S. Knowles, *Acc. Chem. Res.* **1983,** *16,* 106 (see also the special issue of Chemical Reviews entitled *Enantioselective Synth.* **1992,** *5*).

[2] R. Noyori, *Chimia* **1986,** *42,* 215; T. Ohta, H. Takaya, M. Kitamura, K. Nagai, R. Noyori, *J. Org. Chem.* **1987,** *52,* 3176; J. M. Brown, A. P. James, *J. Chem. Soc., Chem. Commun.* **1987,** 181; B. D. Vineyard, W. S. Knowles, M. J. Sabacky, G. L. Bachman, D. J. Weinkauff, *J. Am. Chem. Soc.* **1977,** *99,* 5946.

[3] J. P. Farr, M. M. Olmstead, N. M. Rutherford, F. E. Wood, A. Balch, *Organometallics* **1983,** *2,* 1758; J. P. Farr, M. M. Olmstead, C. H. Hunt, A. L. Balch, *Inorg. Chem.* **1981,** *20,* 1182; E. Farnetti, G. Nardin, M. Graziani, *J. Chem. Soc., Chem. Commun.* **1988,** 1264; M. M. Tacqui Khan, V. V. S. Reddy, H. C. Bajaj, *Inorg. Chim. Acta* **1987,** *130,* 163.

[4] T. Hayashi, M. Konishi, M. Kukushima, K. Kanehira, T. Hioki, M. Kumada, *J. Org. Chem.* **1983,** *48,* 2195, and ref. cit. therein.

[5] a) T. Hayashi, M. Sawamura, Y. Ito, *Tetrahedron* **1992,** *48,* 1999; b) M. Sawamura, Y. Ito, T. Hayashi, *Tetrahedron Lett.* **1990,** *31,* 2723; c) Y. Ito, M. Sawamura, E. Shirakawa, K. Hayashizaki, T. Hayashi, *ibid.* **1988,** *29,* 235; d) M. Sawamura, Y. Ito, T. Hayashi, *ibid.* **1989,** *30,* 2247; e) T. Hayashi, M. Sawamura, Y. Ito, *ibid.* **1988,** *29,* 6321; f) Y. Ito, M. Sawamura, E. Sirkawa, K. Hayashizaki, T. Hayashi, *ibid.* **1988,** *44,* 5253; g) Y. Ito, M. Sawamura, M. Kabayashi, T. Hayashi, *ibid.* **1988,** *29,* 239; h) Y. Ito, M. Sawamura, E. Sirakawa, E. Hayashizaki, K. Hayashi, *ibid.* **1988,** *29,* 235; i) Y. Ito, M. Sawamura, T. Hayashi, *ibid.* **1987,** *28,* 6215; j) Y. Ito, M. Sawamura, T. Hayashi, *J. Chem. Soc., Chem. Commun.* **1986,** *108,* 1090.

[6] a) A. Togni, S. D. Pastor, *J. Org. Chem.* **1990,** *55,* 1649; b) S. D. Pastor, A. Togni, *Helv. Chim. Acta* **1991,** *74,* 905; c) A. Togni, S. D. Pastor, G. Rihs, *J. Organomet. Chem.* **1990,** *381,* C21; d) A. Togni, S. D. Pastor, *Helv. Chim. Acta* **1989,** *72,* 1038; e) A. Togni, S. D. Pastor, *Tetrahedron Lett.* **1989,** *30,* 1071; f) A. Togni, R. Häusel, *Synlett* **1990,** 633.

[7] R. E. Merrill, *Chem. Tech.* **1981,** *11,* 118, and ref. cit. therein.

[8] a) U. Nagel, B. Rieger, *Organometallics* **1989,** *8,* 1534; b) E. P. Kyba, R. E. Davis, P. N. Juri, K. R. Shirley, *Inorg. Chem.* **1981,** *20,* 3616; c) J. D. Oliver, D. P. Riley, *Organometallics* **1983,** *2,* 1032.

[9] A. Albinati, C. J. Ammann, P. S. Pregosin, H. Rüegger, *Organometallics* **1991,** *10,* 1800; P. S. Pregosin, F. Wombacher, *Magn. Reson. Chem.* **1991,** *29,* 106.

[10] K. Wüthrich, in 'NMR of Proteins and Nucleic Acids', Wiley, New York, 1986, and ref. cit. therein.

[11] H. Rüegger, R. W. Kunz, C. J. Ammann, P. S. Pregosin, *Magn. Reson. Chem.* **1991,** *29,* 197; C. J. Ammann, P. S. Pregosin, H. Rüegger, A. Albinati, F. Lianza, R. W. Kunz, *J. Organomet. Chem.* **1992,** *423,* 415.

[12] A. Albinati, F. Lianza, H. Berger, P. S. Pregosin, H. Rüegger, R. W. Kunz, *Inorg. Chem.* **1993,** *32,* 478.

[13] T. C. Appleton, H. C. Clark, L. E. Manzer, *Coord. Chem. Rev.* **1973,** *10,* 335.

[14] P. Hitchcock, B. Jacobson, A. Pidcock, *J. Chem. Soc., Dalton Trans.* **1977,** 2043.

[15] M. Motschi, P. S. Pregosin, L. M. Venanzi, *Helv. Chim. Acta* **1979,** *62,* 667; H. Motschi, C. Nussbaumer, P. S. Pregosin, F. Bachechi, P. Mura, L. Zambonelli, *ibid.* **1980,** *63,* 2071.

[16] R. W. Cullen, T. Kim, F. W. B. Einstein, T. Jones, *Organometallics* **1985,** *4,* 346.

[17] a) N. C. Payne, D. W. Stephan, *Inorg. Chem.* **1982,** *21,* 182; b) M. Cocivera, G. Ferguson, B. Kaitner, F. J. Lalor, D. J. O'Sullivan, M. Parvez, B. Ruhl, *Organometallics* **1982,** *1,* 1132.

[18] a) K. Toriyumi, T. Ito, H. Takaya, T. Souchi, R. Noyori, *Acta Crystallogr., Sect. B* **1982,** *38,* 807; b) A. Miyashita, A. Yasuda, H. Takaya, K. Toriyumi, T. Ito, T. Souchi, R. Nyori, *J. Am. Chem. Soc.* **1980,** *102,* 7932.

[19] R. E. Davis, B. B. Meyer, K. L. Hassett, P. N. Juri, E. P. Kyba, *Acta Crystallogr., Sect. C* **1984,** *40,* 21.

[20] R. G. Ball, N. C. Payne, *Inorg. Chem.* **1977,** *16,* 1187.

[21] A. S. C. Chan, J. J. Pluth, J. Halpern, *Inorg. Chim. Acta* **1979,** *37,* L477; A. S. C. Chan, J. J. Pluth, J. Halpern, *J. Am. Chem. Soc.* **1980,** *102,* 5952.

[22] B. McCulloch, J. Halpern, M. R. Thompsom, C. R. Clark, *Organometallics* **1900,** *9,* 1392.

[23] H. Colquhoun, S. M. Doughty, J. F. Stoddar, A. M. Z. Slawin and D. J. Williams, *J. Chem. Soc., Dalton Trans.* **1986,** 1639.

[24] D. Selen, D. Scharfenberg-Pfeiffer, G. Reck, R. Taube, *J. Organomet. Chem.* **1991,** *415,* 417.

[25] P. S. Pregosin, in 'Phosphorus-31 NMR Spectroscopy in Stereochemical Analysis', Eds. J.-G. Verkade and L. D. Quin, VCH Deerfield Beach, Fla. 1987, Vol. 8, p. 465, and ref. cit. therein.

[26] A. Albinati, S. Affolter, P. S. Pregosin, *Organometallics* **1990,** *9,* 379; C. Ammann, P. S. Pregosin, A. Scrivanti, *Inorg. Chim. Acta* **1989,** *155,* 217; H. Rüegger, P. S. Pregosin, *Inorg. Chem.* **1987,** *26,* 2912.

[27] J. Ni, C. P. Kubiak, *Inorg. Chem.* **1990,** *29,* 4345.
[28] M. J. Hampden-Smith, H. Rüegger, *Magn. Reson. Chem.* **1989,** *27,* 1107.
[29] C. Ammann, P. S. Pregosin, H. Rüegger, M. Grassi, A. Musco, *Magn. Reson. Chem.* **1989,** *27,* 355.
[30] E. W. Abel, N. J. Long, K. G. Orell, A. G. Osborne, V. Sik, P. A. Bates, M. B. Hursthouse, *J. Organomet. Chem.* **1990,** *383,* 253, *ibid.* **1989,** *367,* 275.
[31] E. W. Abel, T. P. J. Coston, K. G. Orrell, V. Sik, *J. Chem. Soc., Dalton Trans.* **1990,** 49; *ibid.* **1989,** 711; E. W. Abel, T. P. J. Coston, K. M. Higgins, K. G. Orrell, V. Sik, T. S. Cameron, *ibid.* **1989,** 701, and ref. cit. therein.
[32] D. Imhof, H. Rüegger, L. M. Venanzi, T. Ward, *Magn. Reson. Chem.* **1991,** *29,* 73.
[33] G. Szalontai, P. Sandor, J. Bakosk, *Magn. Reson. Chem.* **1991,** *29,* 449.
[34] W. E. Hull, in 'Two-Dimensional NMR Spectroscopy, Applications for Chemists and Biochemists', Eds. W. R. Crossmun and R. M. K. Carlson, VCH, Deerfield Park, Fla., 1987, p. 67.
[35] J. Neeser, J. M. J. Trochet, E. J. Charollais, *Can. J. Chem.* **1983,** *61,* 2112.
[36] L. D. Quin, M. J. Gallagher, G. T. Cunkle, D. B. Chesna, *J. Am. Chem. Soc.* **1980,** *102,* 3136.
[37] G. Adlwidjaja, B. Meyer, J. Thiem, *Z. Naturforsch., B* **1979,** *34,* 1547.
[38] X. Han, H. Ruegger, *Planta Med.* **1992,** *58,* 449.
[39] D. B. Davies, 'Progress in Nuclear Magnetic Resonance Spectroscopy', Pergamon Press. Ltd., Oxford, 1978, Vol. 12, p. 135.
[40] a) H. Rüegger, *Magn. Reson. Chem.* **1991,** *29,* 113; b) M. Bortolin, U. E. Bucher, H. Rüegger, L. M. Venanzi, A. Albinati, F. Lianza, S. Trafimenko, *Organometallics* **1992,** *11,* 2514.
[41] B. Schmid, L. M. Venanzi, T. Gerfin, V. Gramlich, F. Mathey, *Inorg. Chem.* **1992,** *31,* 5117.
[42] B. E. Mann, B. E. Taylor, '^{13}C NMR Data for Organometallic Compounds', Academic Press, London, 1981; P. W. Clark, P. Hanisch, A. J. Jones, *Inorg. Chem.* **1979,** *18,* 2067; N. Platzer, N. Goasdone, R. Bonnaire, *J. Organomet. Chem.* **1978,** *160,* 455.
[43] G. M. Sheldrick, SHELX-76 Programs for Crystal Structure Determination, University of Cambridge, 1976, unpublished.
[44] C. K. Johnson, ORTEP II Thermal Ellipsoid Plot Program, Oak Ridge, 1976.